A Spectrotemporal EEG Mapping Approach for Decoding Imagined Marathi Language Phonemes

Umesh Mhapankar

Agnel Charities' Fr. C. Rodrigues Institute of Technology, India
mhapankar.umesh@fcrit.ac.in (corresponding author)

Milind Shah

Agnel Charities' Fr. C. Rodrigues Institute of Technology, India
milind.shah@fcrit.ac.in

ABSTRACT

Individuals facing verbal communication impairments resulting from brain disorders like paralysis or autism encounter significant challenges when unable to articulate speech. This research proposes the design and development of a wearable system capable of decoding imagined speech using electroencephalogram (EEG) signals obtained during the mental process of speech generation. The system's main objective is to offer an alternative communication method for individuals who can hear and think but face challenges in articulating their thoughts verbally. The design suggested includes user-friendliness, wearability, and comfort for seamless integration into daily life. A minimal number of electrodes are strategically placed on the scalp to minimize invasiveness. Achieving precise localization of the cortical areas responsible for generating the EEG patterns during imagined speech is vital for accurate decoding. Literature studies are utilized to determine the cortical positions associated with speech processing. Due to the inherent limitations in EEG spatial resolution, meticulous experiments are conducted to map the scalp positions onto their corresponding cortical counterparts. Specifically, we focus on identifying the scalp location over the superior temporal gyrus (T3) using the internationally recognized 10-20 electrode placement system by employing a circular periphery movement with a 2 cm distance increment. Our research involves nine subjects spanning various age groups, with the youngest being 23 and the oldest 65. Each participant undergoes ten iterations, during which they imagine six Marathi syllables. Our work contributes to the development of wearable assistive technology, enabling mute individuals to communicate effectively by translating their imagined speech into actionable commands. This innovation ultimately enhances their social participation and overall well-being.

Keywords-EEG; imagined speech; location mapping; Wernicke area

I. INTRODUCTION

Speech plays a vital role in human communication; however, a portion of the population may be mute due to brain disorders. Despite possessing the ability to listen, hear, and internally imagine speech, these individuals are unable to overtly reproduce it. About 10% of the global population is affected by such brain disorders [1], emphasizing the pressing need for a non-invasive system capable of decoding internally generated speech. Several methods exist for measuring the brain's activity, including invasive techniques such as Electrocorticography (ECoG) and non-invasive approaches like electroencephalography (EEG). While ECoG offers superior spatial and temporal resolution, it requires surgical intervention and lacks portability. In contrast, with its good temporal resolution, non-invasiveness, and portability, EEG has gained significant traction in applications, such as Brain-Computer Interfaces (BCIs) and clinical settings [2]. Other non-invasive methods to test brain activity are fMRI (functional Magnetic Resonance Imaging) and PET (Positron Emission Tomography) scans, but these techniques have poor temporal resolution and are not portable.

This research focuses on the non-invasive decoding of imagined speech, also known as covert speech, using an EEG system. However, the EEG signals acquired from the scalp are weak, on the order of micro-volts. They are susceptible to contamination from various body artifacts like electrocardiogram (ECG) and electromyogram (EMG) signals, as well as from electromagnetic interference (EMI) signals. Clinical methods employ a minimum of 24 to 64 electrodes using the standard international 10-20 system with wet electrodes and many systems are within the 0-40 Hz bandwidth.

II. RELATED WORK

A. Wernicke area

The existing literature highlights the significance of specific brain regions in language processing. Wernicke area, located in the Superior Temporal Gyrus (STG), as shown in Figure 1, is known to play a crucial role in comprehension. Additionally, the angular gyrus and Broca area, supported by motor neurons, contribute significantly to language articulation prior to real-time speech. These regions collectively assist the pre-processing stages of speech within the brain.
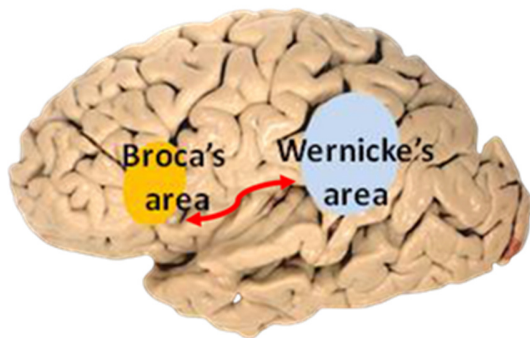

Fig. 1.   Broca and Wernicke areas.

The dorsal stream is surrounded by the lateral sulcus, Broca area, and Wernicke area. The superior longitudinal fasciculus/arcuate fasciculus is the major fiber tract of the dorsal stream. It comprises four subcomponents (superior longitudinal fasciculus I–III), with the arcuate fasciculus constituting the fourth subcomponent. The superior longitudinal fasciculus III and arcuate fasciculus play a significant function in the dorsal language stream.
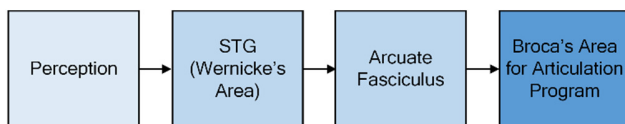

Fig. 2.   Wernicke–Geschwind model.

B. Electrical Dipole at the Superior Temporal Gyrus (STG) due to Speech and other Activities

Many researchers agree that electrical dipoles arise from the dynamic activity in the brain. These dipoles are likely created by a moment that correlates with both location and strength of the activity [3]. However, this potential is reduced when reflected on the scalp due to its layers and the skull's high resistance. For cognitive activity in the brain, the dual-stream model, the dorsal and the ventral is conceptualized in [4]. Understanding the current density and potential development in specific brain areas is crucial for analyzing various activities related to synapses, membranes, fluids, and tissues. In particular, the STG, also known as Wernicke area, plays a vital role in speech comprehension [5].

Figure 3 highlights the STG area, which is responsible for speech comprehension. The electrical dipole influences in this area arise from various activities and can be analyzed using the superposition principle, similar to network theory. The location was selected using the theory mentioned in anatomy books [3]. The potential developed at the STG is influenced by current vectors E_1, E_2, E_3, up to E_n and the potential due to local speech activity. These vectors possess different amplitudes, directions, and phases. The vectors can be separated and analyzed using Independent Component Analysis (ICA). Apart from speech signals, the remaining signals are considered Event-Related Potentials (ERP). These signals are characterized by low frequency and delayed responses hence they do not affect the speech signals. The envelopes for speech signals also exhibit low-frequency characteristics, allowing separating the speech information using spectral filtering, particularly in the gamma and theta frequency ranges. To map the electrical dipole at the STG onto the scalp, a three-sphere model (scalp, skull, and CSF) or a four-sphere model (including the inner brain or cortex) is considered to account for volume conduction as displayed in Figure 4. The placement of electrodes within this boundary is determined by calculations based on Poisson's theorem.
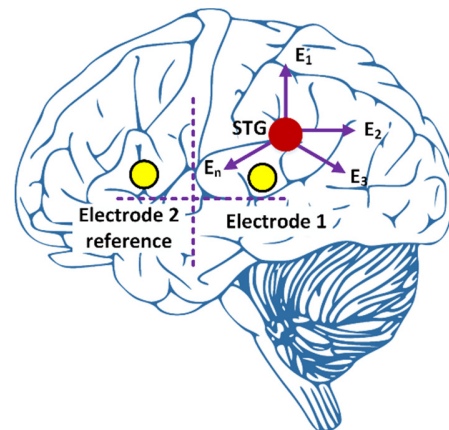

Fig. 3.   Electrode positioning as fMRI, standard 10-20 method on the scalp.
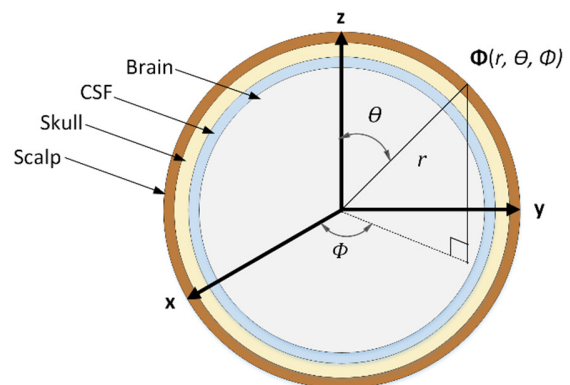

Fig. 4.   A schematic representation of the brain, depicting four layers: the brown-coloured scalp layer, the yellow-coloured skull layer, the light blue-coloured cerebrospinal fluid (CSF), and the light gray-coloured inner brain or cortex. Spherical coordinates ($r, \theta, \emptyset$) are used to represent the location of the STG.

$$\Phi = \sum_1^n E_n e^{-i\omega_n \theta_n} \qquad (1)$$

In (1), E_n is the amplitude of potential due to various inputs, ω_n is the frequency, θ_n is the phase angle of the vector, and n is the number of sources that influence the location at the cortex, involved in speech comprehension. Equation (1) suggests that multiple inputs contribute to the potential with different frequencies and phase components. After acquiring EEG at the proposed location, Fast Fourier Transform (FFT) determines the frequency spectrum, which is then filtered using various bandpass filters through LabVIEW. The resulting drop in potential will be dependent on the equivalent circuit portrayed in Figure 5. Impedance $Z_c + Z_{sk} + Z_{sc}$ will attenuate the voltage at the scalp. The EEG voltage V_{ee} in (2) is given by:

$$V_{ee} = I_s R_t - Z_t I \qquad (2)$$

where I_s is the source current, R_t is the source internal resistance, Z_t is the total impedance including electrode and contact resistance ($Z_c + Z_{sk} + Z_{sc}$), and I is the total current. Before analysis in the LabVIEW, the signal is amplified using a front-end amplifier.
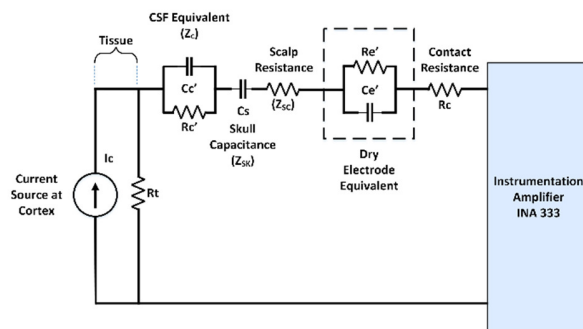

Fig. 5.   Equivalent circuit from cortex to electrode.

C. Electrodes

The choice of electrode type is another critical consideration. Wet Ag/AgCl electrodes are considered the gold standard due to their superior conductivity. However, their application necessitates the use of conductive gel to minimize the contact resistance between skin and electrodes. There are two issues with the gel. First, it creates discomfort for the user, and it dries every five hours, so it needs to be replaced to maintain conductivity [6]. This reduces the system's portability. Additionally, the bandwidth of existing EEG systems poses limitations, as decoding imagined speech requires access to theta waves (0-4 Hz) and high gamma signals (70 Hz-200 Hz and above). To address bandwidth and wet electrode issues, a graphene-coated dry electrode has been developed [7]. Graphene is a highly conducting and sensitive engineering material. These electrodes introduce capacitive reactance into the circuit, creating a high-pass filter to address the low bandwidth nature of the dry electrodes. Additionally, it offers low skin contact resistance, exhibiting characteristics closely resembling the gold standard.

During the mapping process, EEG signals are influenced by low-pass filtering from the cortex to the scalp. Therefore, an expanded bandwidth is essential, posing a challenge for the current EEG systems. ECoG, an invasive technique involving electrode placement on the cortex via surgery, can accurately decode imagined speech, specifically targeting the STG. However, the ECoG method is unsuitable for general wearable applications due to its invasive nature [3, 6]. To address these challenges, this study aims to map the specific scalp region associated with decoding imagined speech using EEG. By accurately projecting the cortex data onto the scalp, we aim to reduce the number of electrodes required. Minimizing the electrode count is a crucial step towards achieving a practical and user-friendly decoding technique. While some researchers have utilized multiple electrodes across the head periphery, others have employed a minimum of 14 channels (electrodes) for EEG-based decoding. Improving the placement of these electrodes based on precise scalp mapping derived from cortex data [8] will contribute to more efficient decoding techniques.

D. Localization

Brain activity signals exhibit three-dimensional characteristics with respect to the normal vector of the activity source. One of the locations where these signals are reflected is the scalp. However, the reflected signal captured by the EEG on the scalp suffers from poor spatial resolution. Therefore, it becomes imperative to accurately map the precise location of the brain activity [9, 10]. The exact localization of primary and secondary speech areas is still being under research [5]. The design should be user-friendly for precise electrode placement on the scalp with minimal electrodes. The literature on localization presents varying perspectives on mapping brain activity and the abstraction of neurons. A widely accepted perspective is based on the modular theory, suggesting that distinct brain regions handle specific tasks and activities, exerting control over corresponding areas of the body [3, 11]. Conversely, some researchers propose a modified perspective, indicating that brain organization may vary across individuals [12]. Furthermore, the literature also delves into the auditory processing pathway within the brain, which elicits differing opinions regarding its course. Two distinct viewpoints emerge: the dorsal and ventral pathways [12-14]. Understanding the precise localization of the electrical potential resulting from speech within the brain's cortex is of utmost importance. This process entails source localization, involving the identification of the cortical region responsible for generating the electrical signal, followed by mapping the same signal onto the scalp for further analysis and interpretation.

Researchers have noticed similarities between the signal properties observed at the cortex and the scalp, apart from differences in bandwidth [15, 16]. While these properties have been primarily investigated in clinical contexts, their confirmation of cognitive activity remains uncertain. Consequently, decoding speech signals necessitates further investigation into the scalp's location. Mapping from the cortex to the scalp is essential as it addresses the issue of volume conduction, as numerous simultaneous activities can influence speech-related activity, making it challenging to isolate clear speech signals. The inter-individual variations in head geometry need also to be considered. It is crucial to study EEG signals simultaneously in the vicinity of the speech location, as indicated in the literature. Such investigations, conducted with

an appropriate experimental setup can provide further evidence to support the correlation between cortical activity and EEG signals during speech-related activities. However, a comprehensive study involving simultaneous analysis of both cortical and EEG activity falls beyond the scope of the study. Instead, this study focuses on conducting multiple iterations of EEG measurements on a diverse group of subjects spanning different age groups and possessing varying head structures.

III. MATERIALS AND METHODS

A. Participants

Nine male participants within the age group of 23 to 65 were selected for this study. All participants had bald heads and no known medical history. The experiments were conducted with the guidance of medical practitioners at Niramay Clinic in Panvel (MS India). Prior to participating in the study, all participants provided an informed consent.

B. Data Acquisition

The experiments utilize multiple electrode placements at different locations to accurately capture speech-related activity. Various speech prompts involving vowels and consonants were utilized, and statistical features as well as spectrotemporal traits were extracted from the EEG data to facilitate analysis. EEG data were recorded using a 32-channel Medicaid, Chandigarh EEG machine with a bandwidth of 512 Hz. Six electrodes were placed on the scalp according to the standard 10-20 electrode placement system, as depicted in Figure 1. The chosen electrode positions were between the T3 (Temporal) and F5 (Frontal) areas. During the recording session, the subjects were instructed to perform three modalities: no speech, overt speech, and imagined speech (covert speech), each lasting for 10 seconds. A total of six Marathi phonemes, including three vowels and three consonants, were used to test the results. They were asked to pronounce the Marathi phoneme [kə] [17] ten times within a duration of 10 seconds, following a one-second starting cue. Subsequently, they were instructed to speak the phonemes [tsə] and [jə], and three vowels [ə], [i], and [u] for a total duration of 90 seconds, with a 5-second break between each set of phonemes. Out of the six, only the [tsə] phoneme was used for location validation, while the other five were utilized for classification purposes.

The acquired EEG data were processed employing the LabVIEW software from National Instruments. Initially, a 50 Hz notch filter was applied to remove power-line artifacts. The data were then filtered putting into service a high-order bandpass filter with a sampling frequency of 512 Hz, to extract five distinct frequency bands: 0-4 Hz (Theta wave), 4-8 Hz (Delta wave), 8-12 Hz (Alpha wave), 12-20 Hz (Beta wave), and 70-200 Hz (Gamma wave). The experiments were conducted implementing two types of electrodes: conventional wet Ag/Ag-Cl electrodes and graphene-based dry electrodes [15].

IV. RESULTS AND DISCUSSION

Experimentation was conducted to confirm the location using nine healthy subjects. Graphene-based 6 cm^2 dry electrodes [18] were selected due to their larger bandwidth compared to wet and other dry electrodes. Power Spectral Density (PSD) was measured, in every iteration, and the average was calculated. PSD was calculated using the Welch method with a Hanning window technique, as illustrated in Tables I-V. The standard deviation indicates that the gamma wave (70-200 Hz) and theta (0-4 Hz) wave have distinct variations compared to other features like delta, alpha, and beta for different prompts. However, the standard deviation for the same prompt across various subjects is insignificant for theta and gamma waves. The bar graphs (Figures 6-9) visualize the results.

The average PSD is highest for all participants at location L1, with minimum deviation for the gamma and theta frequency range. Observations infer that Location 1 provides a more robust output for theta and gamma signals. Location P1 is considered normal with the minimum distance to STG [18], and the standard deviation is lower at the same position. Location P1 exhibits an average PSD higher than the other five locations. Delta, alpha, and beta waves gave inconclusive results because alpha and beta waves arrived with artifacts arising from other activity. The FFT shows a similar gamma frequency range for different participants for the same prompt, and spectrogram features offer similar spectral visualizations for actual classification. The spectrogram of gamma waves (Figure 10) also provides important information about the prompt, which can be further used for regression and classification. Machine learning algorithms like Support Vector Machines and Random Forest, can be utilized to check classification accuracy [19-21].

TABLE I. SD AND AVPSD FOR LOCATION 1

Type of EEG signal	Theta	Delta	Alfa	Beta	Gamma
	0-4 Hz	4-8 Hz	8-12 Hz	12-20 Hz	70-200 Hz
Modality	(SD) AvPSD	(SD) AvPSD	(SD) AvPSD	(SD) AvPSD	(SD) AvPSD
Without speech	(0.23) 2.56	(0.28) 2.91	(0.11) 2.15	(0.17) 3.92	(0.07) 0.24
Overt /[tsə]	(0.11) 5.77	(0.21) 2.51	(0.19) 2.62	(0.14) 3.42	(0.08) 3.68
Covert /[tsə]	(0.14) 4.64	(0.13) 1.75	(0.21) 1.68	(0.13) 2.31	(0.06) 3.14

TABLE II. SD AND AVPSD FOR LOCATION 2

Type of EEG signal	Theta	Delta	Alfa	Beta	Gamma
	0-4 Hz	4-8 Hz	8-12 Hz	12-20 Hz	70-200 Hz
Modality	(SD) AvPSD	(SD) AvPSD	(SD) AvPSD	(SD) AvPSD	(SD) AvPSD
Without speech	(0.34) 2.89	(0.43) 2.89	(0.29) 2.09	(0.45) 4.67	(0.09) 0.15
Overt /[tsə]	(0.56) 4.12	(0.33) 2.67	(0.34) 2.57	(0.39) 2.57	(0.23) 1.68
Covert /[tsə]	(0.37) 4.19	(0.28) 1.75	(0.36) 1.67	(0.41) 3.12	(0.19) 1.56

TABLE III.   SD AND AVPSD FOR LOCATION 3

Type of EEG signal	Theta	Delta	Alfa	Beta	Gamma
	0-4 Hz	4-8 Hz	8-12 Hz	12-20 Hz	70-200 Hz
Modality	(SD) AvPSD	(SD) AvPSD	(SD) AvPSD	(SD) AvPSD	(SD) AvPSD
Without speech	(0.23) 2.54	(0.19) 1.23	(0.19) 1.92	(0.36) 4.72	(0.15) 0.42
Overt /[tsə]	(0.36) 4.49	(0.23) 2.76	(0.28) 2.72	(0.31) 3.52	(0.32) 1.43
Covert /[tsə]	(0.21) 2.23	(0.13) 1.87	(0.34) 1.47	(0.29) 2.67	(0.14) 0.78

TABLE IV.   SD AND AVPSD FOR LOCATION 4.

Type of EEG signal	Theta	Delta	Alfa	Beta	Gamma
	0-4 Hz	4-8 Hz	8-12 Hz	12-20 Hz	70-200 Hz
Modality	(SD) AvPSD	(SD) AvPSD	(SD) AvPSD	(SD) AvPSD	(SD) AvPSD
Without speech	(0.34) 3.21	(0.32) 2.42	(0.38) 2.72	(0.49) 4.65	(0.23) 0.56
Overt /[tsə]	(0.26) 2.72	(0.39) 2.56	(0.29) 1.67	(0.35) 3.25	(0.34) 1.43
Covert /[tsə]	(0.45) 3.56	(0.67) 1.87	(0.69) 1.565	(0.45) 2.23	(0.28) 2.47

TABLE V.   SD AND AVPSD FOR LOCATION 5

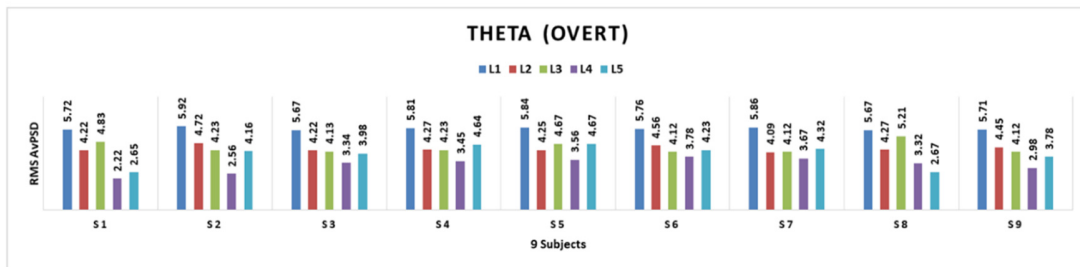| Type of EEG signal	Theta	Delta	Alfa	Beta	Gamma
	0-4 Hz	4-8 Hz	8-12 Hz	12-20 Hz	70-200 Hz
Modality	(SD) AvPSD	(SD) AvPSD	(SD) AvPSD	(SD) AvPSD	(SD) AvPSD
Without speech	(0.21) 3.24	(0.31) 2.75	(0.22) 1.89	(0.45) 4.43	(0.12) 0.56
Overt /[tsə]	(0.26) 3.67	(0.34) 2.45	(0.31) 2.45	(0.32) 2.41	(0.25) 1.39
Covert /[tsə]	(0.26) 3.15	(0.28) 2.76	(0.29) 1.67	(0.27) 2.89	(0.18) 1.12

Fig. 6.   Column chart showing variation RMSAvPSD theta wave for overt speech
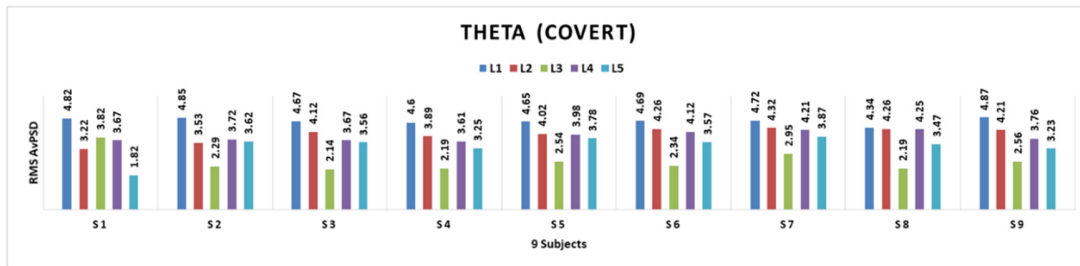

Fig. 7.   Column chart showing variation RMSAvPSD theta wave for covert speech.
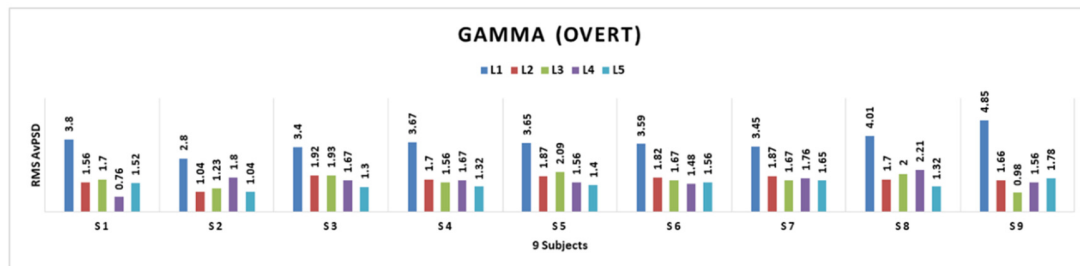

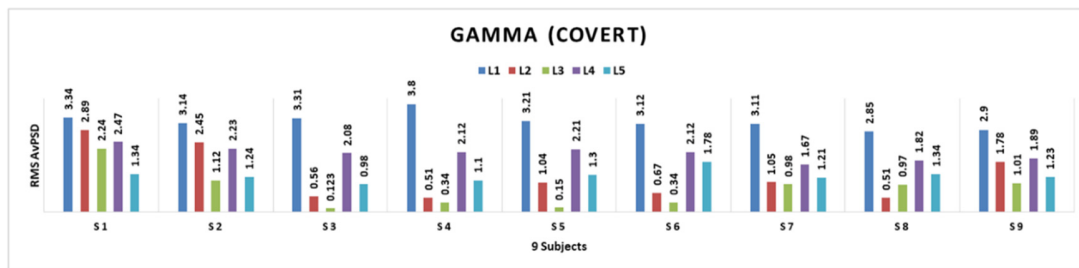Fig. 8.   Column chart showing variation RMSAvPSD gamma wave for overt speech.

Fig. 9.   Column chart showing variation AvRMS PSD theta wave for overt speech.
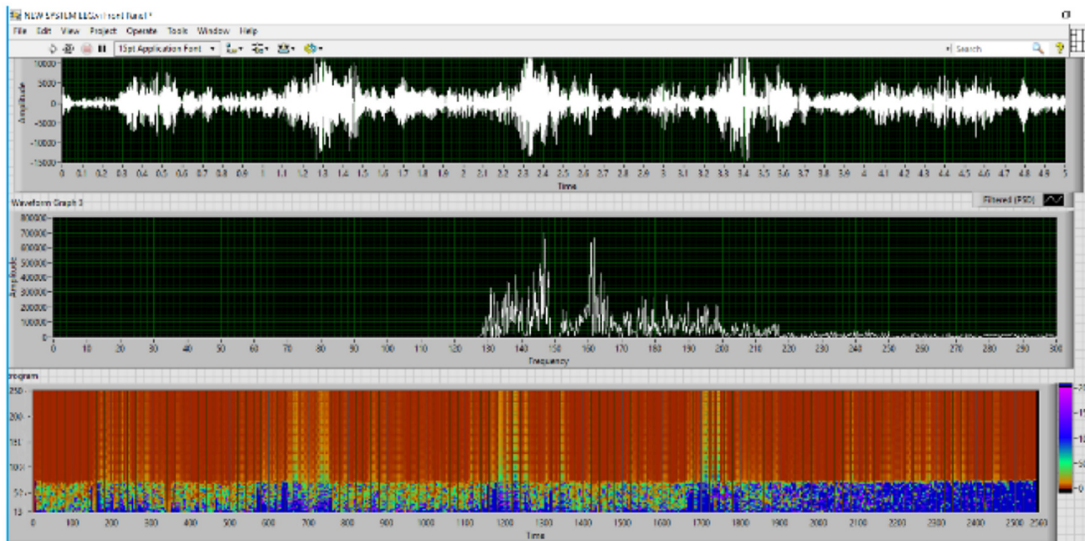

Fig. 10.   Time, FFT, and Spectrogram of Covert [tsə] in Marathi.

V.   CONCLUSION

This study's experimentation using graphene-based dry electrodes and simultaneous measurements from healthy participants has yielded valuable results. The former reveals that selecting an adequate electrode and identifying the location correctly can map speech-like activity on the brain scalp. This observation provides new insights into the intricate dynamics of brain signal localization at various positions on the scalp. The superior temporal gyrus, one of the areas that participate in speech production, can be mapped on the scalp based on head geometry and the international standard of the 10-20 method. Signals on the scalp, specifically the theta and gamma signals, exhibited a significant contribution to speech decoding. The output obtained from this mapping can enhance classification accuracy, as it provides distinct spectrotemporal features. Our work enhances the understanding of the brain's speech-processing capabilities and holds promise for empowering innovative applications in brain-computer interfaces and speech-assistive devices.

REFERENCES

[1]   S. Martin, C. Mikutta, R. T. Knight, and B. N. Pasley, "Understanding and Decoding Thoughts in the Human Brain," *Frontiers for Young Minds*. https://kids.frontiersin.org/articles/10.3389/frym.2016.00004.

[2]   S. Martin *et al.*, "Decoding spectrotemporal features of overt and covert speech from the human cortex," *Frontiers in Neuroengineering*, vol. 7, May 2014, https://doi.org/10.3389/fneng.2014.00014.

[3]   P. L. Nunez and R. Srinivasan, *Electric Fields of the Brain: The Neurophysics of EEG,* 2nd ed. Oxford, UK: Oxford University Press, 2005.

[4]   R. E. Weller, "Chapter 27: Two cortical visual systems in Old World and New World primates," in *Progress in Brain Research*, vol. 75, T. P. Hicks and G. Benedek, Eds. Elsevier, 1988, pp. 293–306.

[5]   J. T. Panachakel and A. G. Ramakrishnan, "Decoding Covert Speech From EEG-A Comprehensive Review," *Frontiers in Neuroscience*, vol. 15, Apr. 2021, Art. no. 642251, https://doi.org/10.3389/fnins.2021.642251.

[6]   S. R. Synigal, E. S. Teoh, and E. C. Lalor, "Including Measures of High Gamma Power Can Improve the Decoding of Natural Speech From EEG," *Frontiers in Human Neuroscience*, vol. 14, 2020, Art. no. 130, https://doi.org/10.3389/fnhum.2020.00130.

[7]   U. Mhapankar and M. M. Shah, "Mapping the Imagined Speech Location on the Brain Scalp Through Magnetoencephalography (MEG)," *International Journal of Recent Technology and Engineering (IJRTE)*, vol. 11, Jul. 2022, https://doi.org/10.35940/ijrte.b7144.0711222.

[8]   U. Mhapankar and M. M. Shah, "Mapping the Imagined Speech Location on the Brain Scalp Through Magnetoencephalography (MEG)," *International Journal of Recent Technology and Engineering (IJRTE)*, vol. 11, Jul. 2022, https://doi.org/10.35940/ijrte.b7144.0711222.

[9]   S. Deng, R. Srinivasan, and M. D'Zmura, "Cortical Signatures of Heard and Imagined Speech Envelopes," Aug. 2013, [Online]. Available:

https://cnslab.ss.uci.edu/speechattention/content/DengSrinivasanDZmura2013.pdf.

[10] J. Derix, O. Iljina, J. Weiske, A. Schulze-Bonhage, A. Aertsen, and T. Ball, "From speech to thought: the neuronal basis of cognitive units in non-experimental, real-life communication investigated using ECoG," *Frontiers in Human Neuroscience*, vol. 8, Jun. 2014, https://doi.org/10.3389/fnhum.2014.00383.

[11] H. Lu, J. Li, L. Zhang, S. S. M. Chan, L. C. W. Lam, and for the Open Access Series of Imaging Studies, "Dynamic changes of region-specific cortical features and scalp-to-cortex distance: implications for transcranial current stimulation modeling," *Journal of NeuroEngineering and Rehabilitation*, vol. 18, no. 1, Jan. 2021, Art. no. 2, https://doi.org/10.1186/s12984-020-00764-5.

[12] B. Oshri, N. Khandwala, and M. Chopra, "Classifying Syllables in Imagined Speech using EEG Data," [Online]. Available: https://cs229.stanford.edu/proj2014/Barak%20Oshri,%20Nishith%20Khandwala,%20Manu%20Chopra,%20Classifying%20Syllables%20in%20Imagined%20Speech%20using%20EEG%20Data.pdf.

[13] A. Borna *et al.*, "A 20-channel magnetoencephalography system based on optically pumped magnetometers," *Physics in Medicine and Biology*, vol. 62, no. 23, pp. 8909–8923, Nov. 2017, https://doi.org/10.1088/1361-6560/aa93d1.

[14] C. Im and J.-M. Seo, "A review of electrodes for the electrical brain signal recording," *Biomedical Engineering Letters*, vol. 6, no. 3, pp. 104–112, Aug. 2016, https://doi.org/10.1007/s13534-016-0235-1.

[15] D. A. Rojas, L. A. Góngora, and O. L. Ramos, "EEGSignal Analysis Related to Speech Process through Bci Device Emotiv, FFT and Statistical Methods," *ARPN Journal of Engineering and Applied Sciences*, vol. 11, no. 5, pp. 3074–3080, 2016.

[16] D. W. Jeong, G. H. Kim, N. Y. Kim, Z. Lee, S. D. Jung, and J.-O. Lee, "A high-performance transparent graphene/vertically aligned carbon nanotube (VACNT) hybrid electrode for neural interfacing," *RSC Advances*, vol. 7, no. 6, pp. 3273–3281, Jan. 2017, https://doi.org/10.1039/C6RA26836F.

[17] "Marathi phonology," *Wikipedia*. Feb. 20, 2024, [Online]. Available: https://en.wikipedia.org/w/index.php?title=Marathi_phonology&oldid=1209133005.

[18] U. Mhapankar and M. Shah, "The Comparison of the Dry Electrodes to wet Ag/AgCI electrode for Decoding Imagined Speech from the EEG," in *2022 International Conference for Advancement in Technology (ICONAT)*, Goa, India, Jan. 2022, pp. 1–6, https://doi.org/10.1109/ICONAT53423.2022.9726038.

[19] M. B. Ayed, "Balanced Communication-Avoiding Support Vector Machine when Detecting Epilepsy based on EEG Signals," *Engineering, Technology & Applied Science Research*, vol. 10, no. 6, pp. 6462–6468, Dec. 2020, https://doi.org/10.48084/etasr.3878.

[20] G. Anuradha and D. N. Jamal, "Classification of Dementia in EEG with a Two-Layered Feed Forward Artificial Neural Network," *Engineering, Technology & Applied Science Research*, vol. 11, no. 3, pp. 7135–7139, Jun. 2021, https://doi.org/10.48084/etasr.4112.

[21] M. A. Alsuwaiket, "Feature Extraction of EEG Signals for Seizure Detection Using Machine Learning Algorthims," *Engineering, Technology & Applied Science Research*, vol. 12, no. 5, pp. 9247–9251, Oct. 2022, https://doi.org/10.48084/etasr.5208.